https://doi.org/10.1016/j.compscitech.2020.108016 **This is the Pre-Published Version.**

Ultrasonic Detection and Characterization of Delamination and Rich Resin in Thick Composites with Waviness

Zhen Zhang[1], Shifeng Guo[2], Qian Li[3], Fangsen Cui[4], Andrew Alexander Malcolm[1], Zhongqing Su[3], Menglong Liu[5*]

[1]Advanced Remanufacturing and Technology Centre, A*STAR *(Agency for Science, Technology and Research)*, Singapore
[2]Shenzhen Key Laboratory of Smart Sensing and Intelligent Systems, Shenzhen Institutes of Advanced Technology, Chinese Academy of Sciences, Shenzhen 518055, China
[3]Department of Mechanical Engineering, The Hong Kong Polytechnic University, Hong Kong Special Administrative Region
[4]Institute of High Performance Computing, A*STAR *(Agency for Science, Technology and Research)*, Singapore
[5]School of Mechanical Engineering and Automation, Harbin Institute of Technology, Shenzhen 518052, P.R. China

[*]Corresponding author: Dr. Menglong Liu email: liumenglong@hit.edu.cn

Abstract: A multi-frequency ultrasonic method was proposed to detect and characterize delamination and rich resin in thick composites with waviness. Addressing the challenges for ultrasonic inspection caused by waviness, multi-layer structure, and multiple defect types, ultrasound propagation in thick wavy composite was investigated through a dedicated numerical model built in OnScale®. Key features of ultrasonic testing and composite sample, including water immersion environment, fiber waviness, uneven inter-ply resin distribution, and side-drilled hole (SDH)-simulated delamination, were embraced in the model. Via this model, waviness and thick resin layers were found to cause disturbance and wave vector deviation to inter-ply reflection signal and thus introduce difficulties for delamination detection based just on the signal to noise ratio. In addition, reflections from inter-ply resin and SDH were revealed with different reliance on probe frequencies. Using a 5 MHz probe with time corrected gain, ultrasonic testing in wavy composite was performed experimentally. Based on the reliance of defect characterization on frequency, SDHs and rich resin were differentiated experimentally in the B-scan images with various filtering frequencies, demonstrating the effectiveness of the proposed method for detection and characterization of delamination and rich resin in thick wavy composite structures.

Keywords: ultrasound, nondestructive evaluation, out-of-plane waviness; composite; delamination

1. Introduction

Carbon fiber reinforced polymer (CFRP) composites are being increasingly used for high-performance

structural applications[1]. Thick composites are widely adopted in aerospace and marine engineering; their rapid expansion is mainly attributed to the improvement of manufacturing techniques. Despite the improvements, fiber waviness, local resin rich region and porosity may still occur in complex-shaped composite structures (e.g., composite fan blade and airfoil)[2]. During the service life, delamination may develop in-between composite layers. The coexistence of multiple defect types increases the risk of composite structural failure and also poses the challenge for defect detection and characterization[3-4].

To extend the service life of composite structures and to reduce the potential failures, non-destructive testing technologies[5-8] including thermography, eddy current, X-ray computed tomography (CT) and ultrasonic testing (UT) are widely used to detect and characterize different defects in composite materials. The UT is the prevailing technology for the detection of surface-breaking, near-surface and sub-surface defects in the composite structures. The main challenges for composite UT inspection are anisotropic properties of composite materials and high attenuation of the UT waves [9-10]. In addition, the multiple layer structure with thin resin layers at the interface, also generates undesirable structural noise [11]. Reported research has demonstrated a good detection capability with UT when only a single defect type like delamination [12], porosity [10] and fiber orientation (in-plane [13] and out-of-plane waviness [14-16]) is present in the composite structures. Wave features like wave attenuation and frequency shift can be used to identify delamination and porosity inside the composites. To evaluate fiber orientation, wave attenuation or phase shift of ultrasound during wave propagation must be mapped with position information using B-scan and C-scan images. Despite numerous applications of UT in composite inspection, delamination within wavy composites is seldom reported to be evaluated with high signal-to-noise ratio (SNR). Local rich resin often develops as waviness blocks the resin movement. Hence both refraction and scattering occur when the ultrasonic wave is propagating through waviness region with thick resin layers. When ultrasonic waves (both longitudinal and shear) propagate through the wavy region and interact with delamination, due to acoustic impedance mismatch between air within delamination and composite material, they will be reflected with possible mode conversion at the delamination [17]. To sum up, the composite inter-ply wave reflection, together with the wave refraction and

scattering caused by waviness, introduces difficulties for defect detection and characterization in composite materials. To improve detection and characterization of delamination and rich resin in composite structures with ultrasound, appropriate signal feature should be discerned and extracted to suppress the interference from waviness.

In order to extract wave features (either in time domain or frequency domain) for defect characterization within composite structures, wave reflection from delamination, waviness and resin rich layers must be fully understood. Ultrasound wavelength has a critical influence on the probability of detecting a discontinuity, including delamination and porosity [18]. A delamination longer than one-half wavelength can reliably be detected by UT [19]. It follows, once the ultrasonic frequency exceeds a certain threshold, detectability of a delamination will be independent of inspection frequency. However, Smith [10] proved with both theoretical and experimental investigation, that inter-ply reflection amplitude of ultrasound is frequency-dependent when propagating in multi-layer composite. The inter-ply reflection reaches maximum when the inspection frequency matches the resonance frequency of single ply. Due to the different frequency dependence of ultrasound reflection of delamination and resin layers, it should be possible to differentiate them in B-scan images at different frequencies.

Despite that, Smith's discovery [10], is built on an ideal model of plane wave incident into flat ply with evenly distributed lamina and inter-ply resin layer along the in-plane direction, and thus no waviness is investigated. While in other works investigating waviness[20], only simplified models with little consideration of inter-ply reflection are established based on ray tracing theory. To sum up, the fine details of a complex structure, including waviness, uneven inter-ply resin, lamina material anisotropy, and defect, can only be addressed via a dedicated numerical model. Nevertheless, the use of numerical models of ultrasound propagation through such a complex composite and their interaction with defect for their characterization has scarcely been addressed. In finite element analysis (FEA), a fine mesh of at least 10 element nodes in one wavelength was advised for homogenous material [21], but the different ply orientation between neighboring plies (usually with thickness 100 μm ~ 200 μm), as well as the inter-ply resin layer (varying from 5 μm to 50

μm), makes the structure heterogeneous to be meshed with extremely small element size. Hence the extremely large consumption of computation resource to tackle all the complex details entails a specialized numerical tool integrated with user-defined structure feature. Typically, Chang et al. [22] used PZflex® to model the propagation of 100 MHz ultrasonic waves through a matrix with fibers, visualizing the complex interactions and dissipation between them. This model demonstrates the superior computation capability of PZFlex®. OnScale®, the successor of PZflex®, with newly developed cloud-based computation, offers a more powerful tool for modeling ultrasound propagation with finite element method. With a further customized model design in this study, the aforementioned details of real thick composite with waviness, material anisotropy, uneven resin layer, and defect is integrated into one model with OnScale® for the first time.

In this study, delamination and rich resin characterization in thick wavy composites with uneven resin distribution is conducted through both numerical modeling and experimental investigation. The principal novelty of this work is the investigation of the effect of the thick resin layers and the out-of-plane waviness on the wave propagation within fiber-reinforced composite. The anisotropic properties of the material due to ply orientation and waviness angle are both taken into account, combined with local rich resin and SDH-simulated delamination. The quantitative dependence of reflection amplitude on the inspection frequency for delamination and thick resin layers in PE mode is obtained numerically and compared with experimental results. It is shown that using the B-scan images formed by the filtered UT signals with different frequencies, delamination can be differentiated from rich resin layers in the waviness region according to both simulation and experimental results.

This paper is organized as follows. In Section 2, the challenge of UT of composite with waviness is briefly addressed, which is followed by an intensive numerical and experimental investigation about the influence of multiple composite features on ultrasound propagation in Section 3. Based on the obtained results from the investigation, three side-drilled holes (SDHs) and local rich resins in a thick composite were inspected and differentiated in Section 4, and final conclusion and discussion are in Section 5.

2. Challenges for UT-based inspection for composites

In this section, the main challenges for UT composite inspection caused by composite internal structure from micro to macro scale will be discussed in detail. Figure 1(a), obtained from optical microscopy, shows thin resin layers (approximately 10 μm) between fiber layers. These resin layers cause inter-ply reflections between the front-wall and the back-wall echoes, when ultrasonic wave propagates in composites. At each interface, for example the interface between layer 1 and 2 as illustrated in Figure 1(a), provided the incident ultrasonic spatial pulse length larger than the ply thickness, there is significant interference to the ultrasonic signal from the neighboring layer 3. This interference is more complex in a typical multi-ply composite. Besides that, the inter-ply reflection will be stronger at resonance if the ultrasonic wavelength matches the odd number of layer thickness.

During manufacturing of aerospace composite structures with a complex shape and a ply drop layout (e.g. composite fan blade and aerofoil), fiber wrinkling can easily convert to either in-plane or out-of-plane waviness due to uneven pressure and heating. These defect types are depicted in Figure 1(b) and (c). As a consequence, the resin flow is blocked in the wavy region and thick resin layers form between the fiber layers. Both magnitude and distribution of waviness and inter-ply resin layer show a strong unevenness and randomness, resulting in the uncertainty of wave scattering intensity and direction at the waviness profile. This uncertainty increases the difficulty of echo signal interpretation.

Material anisotropy presents another challenge for composite UT inspection. In the immersion testing, a complex wave refraction and mode conversion pattern will develop on the water-composite interface depending on the incident angle. This is illustrated in Figure 1(d). If longitudinal waves reach the composite-water interface at the normal incident angle, the only waves that will refract are longitudinal ones. However, a skewed incidence will generate both refracted quasi-longitudinal (QL) and transverse (QT) waves in the composite. Since the multiple refracted waves will continue to interact with the composite layers, very complex signals will be acquired due to the wave reflection, refraction and the mode conversion. Therefore, we limit the investigation in this study to normal incident angle, to reduce the difficulty of signal interpretation and

processing.

The CFRP sample (ply stacking $[0/90]_{26s}$ and sample dimension 15 mm (maximum depth) • 35 mm (length) • 20 mm (width)) with three 2 mm diameter SDHs was prepared. SDHs were drilled to the half width of the sample. The X-ray CT images of the sample are shown in Figure 2. Note that the ply drop layout was used to form the required complex shape. This generated waviness in the 6-10 mm depth range between two relative straight layers region, also shown in Figure 2. Only the top side, straight surface of the sample was accessible for inspection, so PE UT method was used. The cross-section images from different widths, obtained from X-ray CT, show also the out-of-plane waviness and resin rich layers.

The experimental setup for composite inspection, consisting of ScanMaster ultrasonic immersion testing system (LS-50), Olympus ultrasonic probe (5 MHz) and fixtures, is shown in Figure 3(a). Raster scanning with a 0.2 mm pitch was conducted at the same water path as the probe focus depth (2 inches). To overcome the intensive wave attenuation in composite and to suppress system noise, the time-corrected gain (TCG) was used to improve SNR. Surface following technology (i.e., applying the delay laws to keep the water path constant) was adopted to compensate for system vibration during the mechanical scanning.

The B-scan images, built from the raw signals captured in defective regions shown in Figure 2, with/without three SDHs using the 5 MHz probe are displayed for comparison purposes in Figure 3(b) and (c). All three SDHs were detected, but the SDH3 indication at the deepest position displays some profile distortion. In addition, some strong reflections of unknown origin can be seen in the B-scan image (indications D, E, F, and G in Figure 3(b) and some points in Figure 3(c)). From the X-ray images shown in Figure 2, the depth of the thick resin layer was measured to be 2 mm, the same depth that the indications F and G are located at. In addition, the close examination of the X-ray image shows that indication E comes from a small-size delamination. All these structural features and defects are mixed together to form a complex UT B-scan image, which furthermore increases the complexity of defect detection and characterization in composites.

3. Study of ultrasound propagating in wavy composite

To achieve defect detection and characterization in composite material using UT, wave interaction with

different types of defects and features (i.e., delamination, resin rich layer and waviness) must be further investigated. To differentiate delamination from other types of defects based on different interaction patterns between the defects and ultrasonic waves, a quantitative dependence of defects on the wave frequency will be analyzed.

3.1. Effect of resin layer on wave propagation

3.1.1. Simulation model setup

FEA tool OnScale® [23] was adopted for numerical modeling first. To investigate the influence of resin layer on the wave propagation, waviness was first excluded to build a model of flat composite sample. The model was built with thin resin layers (10 μm thickness) between each of the neighboring composite plies, comprising a layup orientation of $[0/90]_{10s}$. One of the thin resin layers was replaced by a thick resin layer (50 μm thickness), between the composite plies 20 and 21. Water was used as the immersion media to transfer the acoustic energy from the transducer into the composite sample. Mesh sizes of 3.33 μm and 10 μm along the thickness and in-plane directions respectively were assigned to guarantee calculation accuracy. To excite and sense ultrasound, one array transducer composed of 36 elements (1.05 mm element pitch and 1 mm element width) was artificially built with the same material as the immersion medium water. Excitation was applied by pressure loading at the middle surface of specified transducer element, and sensing was realized by extracting the pressure signal at the same surface. Hence different excitations were enabled by selecting probe elements at any desired locations. To generate an approximate plane wave normal to the interface between the water and the composite sample, 36 ultrasonic phased array elements were excited simultaneously. The material properties for composite ply, epoxy matrix (resin layers), and water are shown in Table 1.

3.1.2. Results and Discussions

A frequency sweeping $2\ \text{MHz} \leq f \leq 12\ \text{MHz}$ was performed, with the pressure signal averaged from all 36 probe elements in PE mode, as shown in Figure 4(a). As already discussed in Section 2, by using the approximate normal incidence wave, the refracted waves are mainly longitudinal one, simplifying the signal processing and analysis. The reflections from the front wall, the resin layer, and the back wall constitute the

acquired signal. Following the font wall reflection, the thin resin layer reflection is not clearly observed when $f \leq 6$ MHz, and oscillates in the time domain till attenuating to a negligible value when $f > 6$ MHz. In contrast, the thick resin layer reflection is well observed in the investigated frequency domain $2\text{MHz} \leq f \leq 12$ MHz. Hence a quantitative investigation into influence of the resin layer thickness and the probing frequency on echo signal is performed.

Figure 4(b) shows the magnitude ratio of the resin layers with different thicknesses and the front wall reflection signals, plotted as a function of frequency. It is observed that the reflection signal from the thin resin layer is barely noticeable when $f \leq 6$ MHz, and then gradually increases to around 0.15 when $f = 12$ MHz, while the reflection signal from the thick resin layer increases from 0.1 to 0.3 when $2\text{ MHz} \leq f \leq 6$ MHz, and then decreases to around 0.22 when $f = 12$ MHz. Therefore, it can be concluded that the inter-ply reflection magnitude is dependent on ultrasound frequency. Since the thin resin layers are distributed widely in the composite, the induced reflection signals oscillate for a long-time duration before the signal amplitude is negligible. To perform the defect characterization (i.e., differentiate delamination from other defect types) with PE method, the thin resin layer reflections should be suppressed. For this, the frequencies less than 6 MHz are more suitable. Furthermore, the alternating lamina-resin layer structure with different resin layer thickness may have different resonance frequencies. It can also be predicted that with the existence of waviness, inter-ply reflection may become more unpredictable due to the increase of structural complexity.

3.2. Effect of waviness on wave propagation

3.2.1. Simulation model setup

A novel model with the geometrical features resembling the experimental sample shown in Figure 2 was proposed and built with OnScale®. The model embraced a $[0/90]_{26s}$ layup orientation, waviness, the thick resin layer, and the SDHs, in water immersion environment, as shown in Figure 5. Since the ply drop region was located below the SDHs, and therefore would not affect the SDH reflection in the PE mode, to simplify the numerical analysis, ply drop was neglected in this study. In addition, a simplified equivalent waviness profile was modeled above SDHs to qualitatively analyze the influence of the waviness and the thick resin layers on

the wave propagation.

The out-of-plane waviness was constructed with curved plies, whose y location of each ply in the thickness direction can be expressed as

$$y=\begin{cases} y_0, & (y_0 \le \mathrm{u}_y-\frac{1}{2}\lambda_y) \\ y_0 - A(\frac{1}{2}+\frac{1}{2}\cos(\frac{2\pi(\mathrm{u}_y-y_0)}{\lambda_y}))\sin(\frac{2\pi x}{\lambda_x}), & (\mathrm{u}_y-\frac{1}{2}\lambda_y < y_0 \le \mathrm{u}_y+\frac{1}{2}\lambda_y) \\ y_0, & (\mathrm{u}_y+\frac{1}{2}\lambda_y < y_0 \le tkn) \end{cases} \quad (1)$$

where y_0 denotes the coordinate of flat composites without waviness in the thickness direction, and thus $y_0 \rightarrow y$ can be seen as a mapping process between the flat and the curved composite. u_y is the center coordinate of waviness region in the thickness direction. λ_y denotes the entire waviness thickness, and λ_x the wavelength of the waviness along the x direction. A is the displacement magnitude of waviness, and tkn denotes the thickness of the entire composite. Angle α depicts the varying waviness angle in each local area of the composite. For the same ply, multiple contour lines of equal waviness angle are drawn (see the zoom-in plot in Figure 5), with two neighboring lines denoting the 1° angle change. The sample parameters are given in Table 2.

The waviness angle α can be calculated from the derivative dy/dx according to Eq. (1) as

$$\alpha = \arctan(dy/dx)$$

$$=\begin{cases} 0, & (y_0 \le \mathrm{u}_y-\frac{1}{2}\lambda_y) \\ \arctan(-\frac{2\pi A}{\lambda_x}(\frac{1}{2}+\frac{1}{2}\cos(\frac{2\pi(\mathrm{u}_y-y_0)}{\lambda_y}))\cos(\frac{2\pi x}{\lambda_x})), & (\mathrm{u}_y-\frac{1}{2}\lambda_y < y_0 \le \mathrm{u}_y+\frac{1}{2}\lambda_y). \\ 0, & (\mathrm{u}_y+\frac{1}{2}\lambda_y < y_0 \le tkn) \end{cases} \quad (2)$$

Using the geometry parameters from Table 2, three models with different maximum waviness angles 0° (A = 0), 12° (A = 0.5), and 20° (A = 0.86) are built and calculated. Waviness leads to the local rotation of fiber direction, and attributed to the anisotropy of composite, the material principal direction is hence also rotated.

Thus, the stiffness matrix of each ply at each local location is rotated by corresponding angle.

Besides the dedicated model of fiber waviness, resin layers of varying thicknesses between neighboring composite plies were added to the model. Since waved fibers interfere with the resin flow, a thick resin layer is easier to produce in the wavy than in the flat fiber region. Thus, one thick resin layer 50 μm thick (thickness from the sample displayed in Figure 2) was built into the wavy region that had the largest waviness (see the zoom-in plot in Figure 5). In addition, thin resin layers (average thickness 10 μm, close to actual resin layer thickness of the testing sample) were also built between neighboring composites, conforming to the waviness shape. By doing so, the thickness of thin resin layer varied at different waviness region, but with a constant thickness of 10 μm in the flat region. Finally, three SDHs with 2 mm diameter were modeled at the same locations as in the test sample. The small delamination shown in Figure 2 was not modelled, since the wave interaction with delamination and SDHs is similar in the PE mode.

To capture the heterogeneous geometric details for accurate modeling, the same mesh used for modeling of the flat composite is remained, i.e. a size of 3.3 μm and 10 μm was assigned along the thickness and in-plane direction of composite, respectively. In this manner, at least three elements were discretized for most inter-ply resin regions, except the ones in the waviness region where the resin layer may have quite small thickness. Same as the case of flat composite, one array transducer composed of 36 elements (0.2 mm element pitch) was artificially built. To investigate the influence of waviness and SDH1 on the wave propagation, in the FEA model probe elements 6 to 11 were excited simultaneously, forming an entire probe length 6.3 mm (same as probe diameter in the experiment), as shown in Figure 5. Central frequency of 5 MHz was used for excitation, in order to avoid strong reflection from the thin resin layer.

3.2.2. Results and discussions

The calculated velocity magnitude contours at different time instants are displayed in Figure 6, which indicate clearly the wave excited by probe (see Figure 6(a)), incident into composite sample (see Figure 6(b)), and scattering from both the thick resin layer and SDH1 (see Figure 6(c) and (d)). The velocity magnitude contour through the waviness region (12° or 20° waviness angle with one layer of 50 μm thick resin therein)

is scattered irregularly over a large area. This is caused by the complex wave refraction and reflection through varied fiber orientation. Attributed to the approximate normal incidence and reflection, the echo signal acquired with the probe can still indicate the existence of SDH1.

To comparatively study the influence of waviness with thick resin layers on the wave propagation, two other numerical models were also built, including (i) flat composite with one layer of 50 μm thick resin and (ii) flat composite with one layer of 20 μm thick resin, and the pressure signals accumulated from the excited six probe elements corresponding to SDH1 were extracted. For comparison, the experimental signals from four cross sections (row 15, 20, 25 and 30 in the raster scanning with each row at a scanning pitch 0.2 mm) in the defective regions with SDH1 were acquired. Normalized pressure signals in both the simulation (see Figure 7(a)) and experiment (see Figure 7(b)) display an almost stable SDH1 scattering signal regardless of differences in waviness shape and resin layer thickness. It is because that acoustic impendence along the normal direction between inter-ply resin and composite ply with carbon fiber (normal to fiber ply direction) is not significantly different, and only a small portion of incident energy is reflected and most is able to transmit through the interface. Nevertheless, the normalized pressure signals in the simulation and experiment both display a significant variation of resin layer wave scattering. Specifically, for waviness with the angles of 12^0 and 20° in the simulation model, both the time-of-flight and the amplitude of the thick resin layer reflection signal change significantly compared to the flat samples without waviness. This change is mainly attributed to the difference of waviness shape and resin layer thickness. For the case of flat composite with one 50 μm thick resin layer, the resin layer wave scattering is much larger in magnitude than the SDH1 scattering, indicating the ineffectiveness to differentiate SDHs from resin layers with magnitude-based signal feature (i.e. SNR).

4. Defect and rich resin characterization for wavy composite

In Section 3.2, it was concluded that the inter-ply reflection amplitude at an excitation with central frequency 5 MHz can even be stronger than SDH reflection, therefore delamination (i.e., SDH) cannot be differentiated from the thick resin layer reflection based on SNR due to uncertain inter-ply reflection caused by waviness accompanied by resin layers with different thickness. In this subsection, it will be attempted to

differentiate the delamination from the thick resin layers, based on the interaction pattern between the defects and the ultrasonic wave, under different frequencies.

4.1. Signal decomposition with SWT

In order to simplify the test procedure that requires multiple probes with different frequencies, the reflected signals with a 5 MHz center frequency from simulation were filtered to signals with different center frequencies from 2.5 MHz to 6 MHz with a 0.5 MHz step using synchrosqueezing wavelet transform (SWT)[24] in MATLAB®. Due to its high time-frequency resolution, SWT was selected to deal with the ultrasound signals consisted of multiple sources of reflection.

The raw and filtered waveform and the related wave packet contour of reflected waves from SDH1 through waviness (maximum waviness angle 12°) and a thick resin layer (50 μm thickness) are shown in Figure 8(a) and (b), respectively. In the raw signal, reflections from both the thick resin layer and the SDH1 are similar, which introduce difficulties for defect characterization based on the SNR. However, in the filtered signals, the signal magnitude of thick resin layer reflection increases with increasing center frequencies. On the other hand, reflection from SDH1 decreases gradually with increasing center frequencies. Therefore, a delamination can be potentially differentiated from a thick resin layer based on the different dependence of defect reflection on the frequency.

4.2. Effect of combined structural feature and SDH on wave reflection signals

To quantitatively analyze the difference of the wave interaction with thick resin layers and with the SDH defects, the magnitude ratios of thick resin layer reflection to the front wall reflection are calculated, including ten simulation and two experimental cases in total. After normalization based on the result at 2.5 MHz, the magnitude ratios are plotted versus center frequencies in Figure 9(a) and (b), respectively. The resin layer reflections display an almost monotonic increase in the flat composite, attributed to the approaching of single ply resonance frequency as the frequency increase. Nevertheless, in the other cases, the resin layer reflections only show a trend of increase featuring a large variation. This indicates that approaching of resonance frequency results in the trend of increase, while the magnitude and distribution randomness of waviness and

inter-ply resin layer leads to the large variation. Particularly, for the cases with a resin layer of 50 μm and waviness angle 20^0 (see "angle 20^0 resin 50 μm SDH1 to SDH3" in Figure 9(a)), the severe magnitude and distribution randomness of waviness and inter-ply resin layer may explain the phenomenon that the reflection peak occurs or stops increasing at around 4.5 MHz, instead of 7 MHz in Figure 4(b)). Another interesting phenomenon is that the magnitude ratio of the resin reflection signal from the case "angle 12^0 resin 50 μm SDH2" remains almost stable throughout the investigated frequencies, which may also result from the complex wave propagation induced by alternating lamina-resin layers with waviness. On the contrary, the normalized magnitude ratios of SDH to front wall reflection signals (see Figure 9(b)) display an almost monotonic decrease with the increase of frequency, well validating the conclusion that resin layer and waviness lead to minor influence on SDH scattering.

To sum up the results, for the flat composite, ultrasound inter-ply rich resin reflection becomes stronger when ultrasound frequency approaches the ply resonance. In the composite with waviness and local rich resin, the inter-ply reflection keeps a trend of increase with frequency increase, but due to the complex wave scattering and deviation at the varied fiber orientations and resin layer thickness, the reflection signal is severely varied at different frequencies. On the contrary, waviness and uneven thick resin layers result in only minor variation into SDH reflection. And SDH reflection almost decreases monotonically with the increasing frequencies. Hence, it is feasible to obtain frequency dependence of defect reflection from the filtered signals through SWT on a raw signal and subsequently for defect characterization.

4.3. Characterization of defect and rich resin

To characterize the volumetric defects (including delamination and SDHs) and differentiate them from local resin rich areas, the formed B-scan images of the composite sample in Section 2 constructed from filtered signals with SWT are shown in Figure 10. From the comparison of B-scans with different center frequencies, it can be seen that at the frequencies below 3 MHz, only SDH indications (indications A, B, C) and indications of the unknown origin (indications D and E), are present in the B-scan images. With the increasing frequencies, these indications become weaker and SDH3 at the deepest position can barely be observed. Intensive

attenuation of high-frequency ultrasound is likely responsible for these changes. On the other hand, the rest highlighted indications (indications F, G) in Figure 3 become stronger with increasing frequencies. Therefore, these indications are likely reflections from the thick resin layers. From the X-ray images shown in Figure 2, the depth of the thick resin layer was measured to be 2 mm, the same depth that the indications F and G are located at.

Based on the reflection dependence of different defects on the ultrasonic frequency, as manifested by the magnitude ratios of defect reflection and front-wall reflection against the filtered frequency shown in Figure 9, the detection and characterization of delamination and rich resin were realized, with the following conclusions drawn:

i) Indications A, B, and C are SDHs, as indicated by the magnitude drops with the increase of the frequency, also supported by the numerical simulation, as shown in Figure 9(b).

ii) Indication D is an artifact from SDH3 (as illustrated with simulated velocity magnitude in Figure 6(d)) possibly due to the waviness-induced wave vector deviation. It only shows at the low frequencies and disappears when the frequency is increased.

iii) The indication E shows the same frequency dependence as delamination. The close examination of the X-ray image shown in Figure 2 supports the assumption that indication E comes from a small-size delamination.

iv) According to the numerical simulation results displayed in Figure 9(b), indications F and G can be attributed to the thick resin layer, since the magnitude increases when the frequency increases.

5. Conclusion and discussion

In this study, the wavy thick composite sample was investigated using numerical modeling and experimental ultrasonic measurements. Challenges for UT inspection caused by multi-layer structure and multiple defect types were identified and described in detail. The effect of the thick resin layers and waviness on the wave propagation was revealed with the dedicated numerical model built in OnScale®. Waviness and thick resin layers were found to introduce additional inter-ply wave scattering, which acts as noise to SDH and

delamination reflection signals, causing difficulties in characterization based only on SNR. The dependences of SDH and thick resin layer reflection magnitudes on frequency were quantitatively analyzed through SWT filtered signals. This showed to be a promising way to reliably detect and characterize delamination and rich resin defects. Making use of different defect reflection magnitude dependence on the ultrasonic frequency, internal delamination and rich resin were successfully detected and characterized. The experimental results were in close agreement with numerical simulation. Due to the difficulties in the modelling of actual composite structures with unpredictable in-plane and out-of-plane waviness, only qualitative comparison between numerical simulation and experimental investigation was conducted. The UT findings were also validated using the X-ray images of the sample. The application of artificial intelligence (AI) for signal processing of UT signals will be a next step in our research, which shows potential to ease operator decision making in defect detection and characterization.

Acknowledgements

This project was partially funded by the National Natural Science Foundation of Guangdong (No. 2016A030313177), Guangdong Frontier and Key Technological Innovation (No. 2017B09-0910013), the Science and Technology Innovation Commission of Shenzhen (Nos. ZDSYS20190902093-209795, JCYJ20170818153048647 and JCYJ-20180507182239617), and the Hong Kong Research Grants Council via General Research Fund (Nos. 15201416 and 15212417). Fangsen Cui wants to thank IHPC for the use of computational resources to carry out this research. Menglong Liu wants to thank Jeff Dobson from OnScale® for the support in numerical simulation. Zhen Zhang wants to thank Bisma Mutiargo and Mato Pavlovic from ARTC for conducting the X-ray CT scans and proof reading.

Reference

[1] Gigante V, Aliotta L, Phuong VT, Coltelli MB, Cinelli P, Lazzeri A. Effects of waviness on fiber-length distribution and interfacial shear strength of natural fibers reinforced composites. Composites Science and Technology. 2017;152:129-138.

[2] Wilhelmsson D, Gutkin R, Edgren F, Asp L. An experimental study of fibre waviness and its effects on compressive properties of unidirectional NCF composites. Composites Part A: Applied Science and Manufacturing. 2018;107:665-674.

[3] Zhang Z, Liu M, Liao Y, Su Z, Xiao Y. Contact acoustic nonlinearity (CAN)-based continuous monitoring of bolt loosening: Hybrid use of high-order harmonics and spectral sidebands. Mechanical Systems and Signal Processing. 2018;103:280-294.

[4] Zhang Z, Xu H, Liao Y, Su Z, Xiao Y. Vibro-acoustic modulation (VAM)-inspired structural integrity monitoring and its applications to bolted composite joints. Composite Structures. 2017;176:505-515.

[5] Yu X, Ratassepp M, Fan Z. Damage detection in quasi-isotropic composite bends using ultrasonic feature guided waves. Composites Science and Technology. 2017;141:120-129.

[6] Garcea S, Wang Y, Withers P. X-ray computed tomography of polymer composites. Composites Science and Technology. 2018;156:305-319.

[7] Hassen AA, Taheri H, Vaidya UK. Non-destructive investigation of thermoplastic reinforced composites. Composites Part B: Engineering. 2016;97:244-254.

[8] Pain D, Drinkwater BW. Detection of fibre waviness using ultrasonic array scattering data. Journal of Nondestructive Evaluation. 2013;32(3):215-227.

[9] Wooh S-C, Daniel IM. Wave propagation in composite materials with fibre waviness. Ultrasonics. 1995;33(1):3-10.

[10] Smith RA. Use of 3D ultrasound data sets to map the localised properties of fibre-reinforced composites. PhD thesis, University of Nottingham, 2010.

[11] Smith RA, Mukhopadhyay S, Lawrie A, Hallett SR. Applications of ultrasonic NDT to aerospace composites. Proceedings of the 5th International Symposium on Aerospace NDT, Singapore, 2013.

[12] Amenabar I, Mendikute A, López-Arraiza A, Lizaranzu M, Aurrekoetxea J. Comparison and analysis of non-destructive testing techniques suitable for delamination inspection in wind turbine blades. Composites Part B: Engineering. 2011;42(5):1298-1305.

[13] Chakrapani SK, Barnard D, Dayal V. Detection of in-plane fiber waviness in composite laminates using guided Lamb modes. AIP Conference Proceedings, vol. 1581: AIP; 2014. p. 1134-1140.

[14] Pain D, Drinkwater BW. Detection of fibre waviness using ultrasonic array scattering data. Journal of Nondestructive Evaluation, Diagnostics and Prognostics of Engineering Systems. 2013;32(3):215-227.

[15] Chakrapani SK, Dayal V, Barnard D, Hsu D. Investigation of Discrete Out-of-Plane Waviness in Composite Wind Turbine Blades Using Ultrasonic Nondestructive Evaluation. ASME 2011 Pressure Vessels and Piping Conference: American Society of Mechanical Engineers; 2011. p. 259-266.

[16] Zardan J-P, Gueudré C, Corneloup G. Study of induced ultrasonic deviation for the detection and identification of ply waviness in carbon fibre reinforced polymer. NDT & E International 2013;56:1-9.
[17] Chakrapani SK, Dayal V, Barnard DJ, Eldal A, Krafka R. Ultrasonic Rayleigh wave inspection of waviness in wind turbine blades: Experimental and finite element method. AIP Conference Proceedings, vol. 1430: AIP; 2012. p. 1911-1917.
[18] Chan V, Perlas A. Basics of ultrasound imaging. Atlas of ultrasound-guided procedures in interventional pain management: Springer; 2011. p. 13-19.
[19] Smith LS, Engeler WE, O'donnell M. Two-dimensional phased array of ultrasonic transducers. Google Patents; 1989.
[20] Kim KY, Zou W, Sachse W. Wave propagation in a wavy fiber–epoxy composite material: Theory and experiment. The Journal of the Acoustical Society of America. 1998;103(5):2296-2301.
[21] Liu M, Schmicker D, Su Z, Cui F. A Benchmark Study of Modeling Lamb Wave Scattering by a Through Hole Using a Time-Domain Spectral Element Method. Journal of Nondestructive Evaluation, Diagnostics and Prognostics of Engineering Systems. 2018;1(2): 021006.
[22] Chang J, Zheng C, Ni Q-Q. The ultrasonic wave propagation in composite material and its characteristic evaluation. Composite Structures. 2006;75(1):451-456.
[23] Dobson J, Tweedie A, Harvey G, O'Leary R, Mulholland A, Tant K, et al. Finite element analysis simulations for ultrasonic array NDE inspections. AIP Conference Proceedings, vol. 1706: AIP Publishing; 2016. p. 040005.
[24] Daubechies I, Lu J, Wu H-T. Synchrosqueezed wavelet transforms: An empirical mode decomposition-like tool. Applied and computational harmonic analysis. 2011;30(2):243-261.

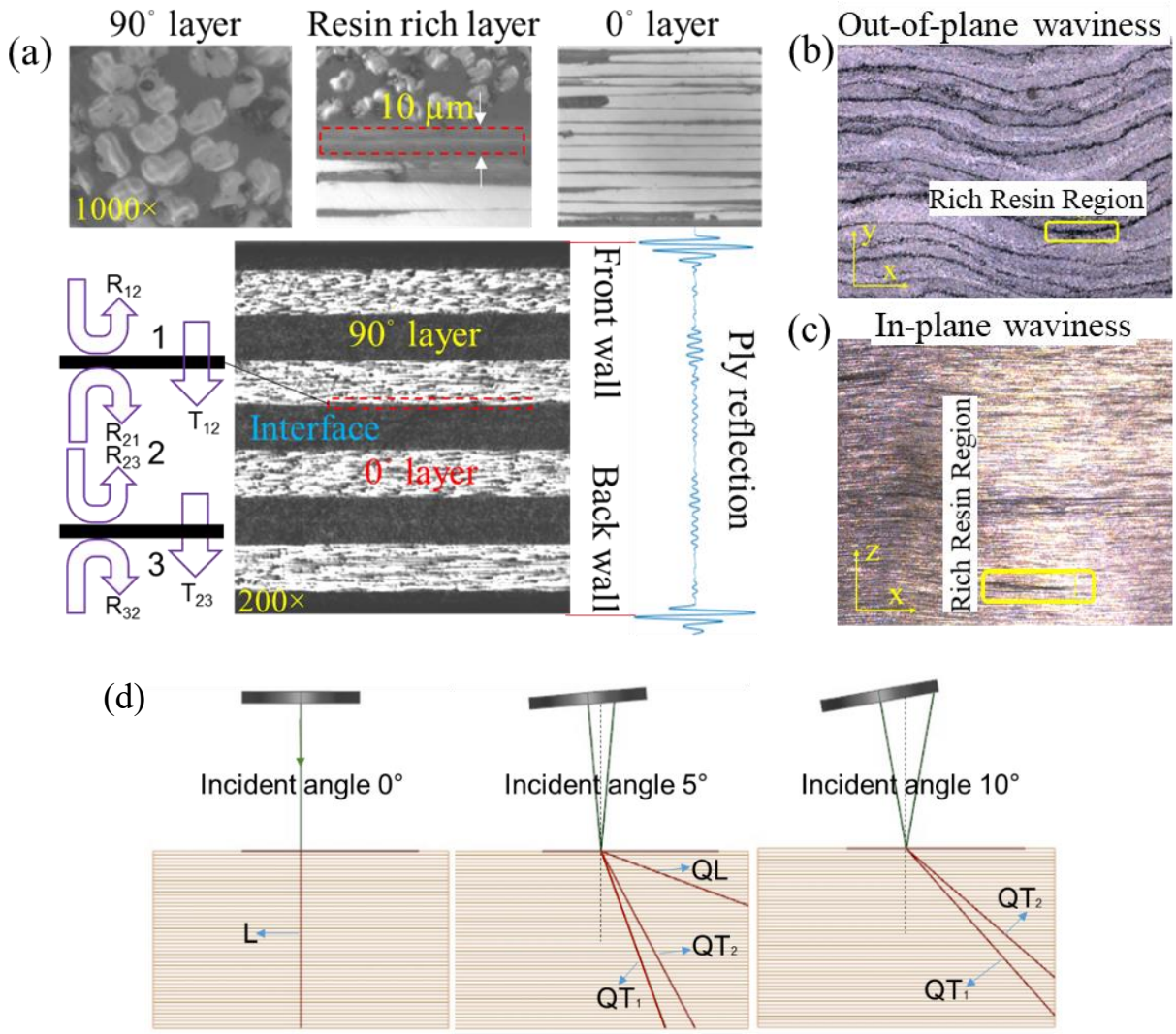

Figure 1. (a) Wave propagation in multi-layer composites, (b) out-of-plane waviness, (c) in-plane waviness within thick composites, and (d) refracted waves at water-composite interface generated at varied incident angles.

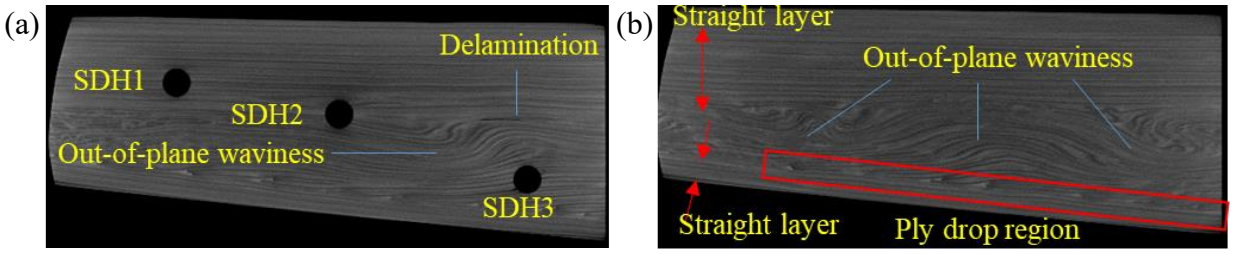

Figure 2. X-ray images of composite cross-section (a) with SDHs and (b) without SDHs.

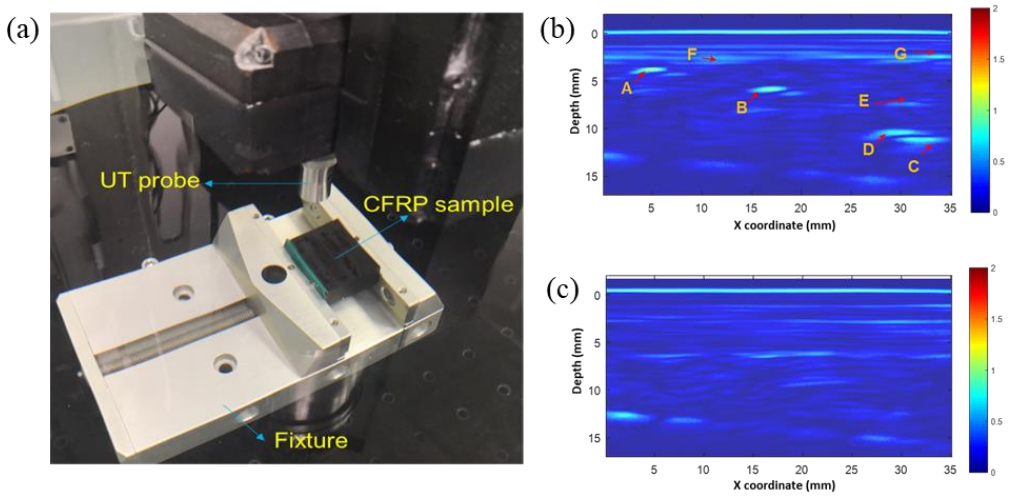

Figure 3. (a) Experimental setup for immersion UT testing, (b) raw B-scan images at position from Figure 2a with three SDHs and, and (c) raw B-scan images at position from Figure 2b without any SDH.

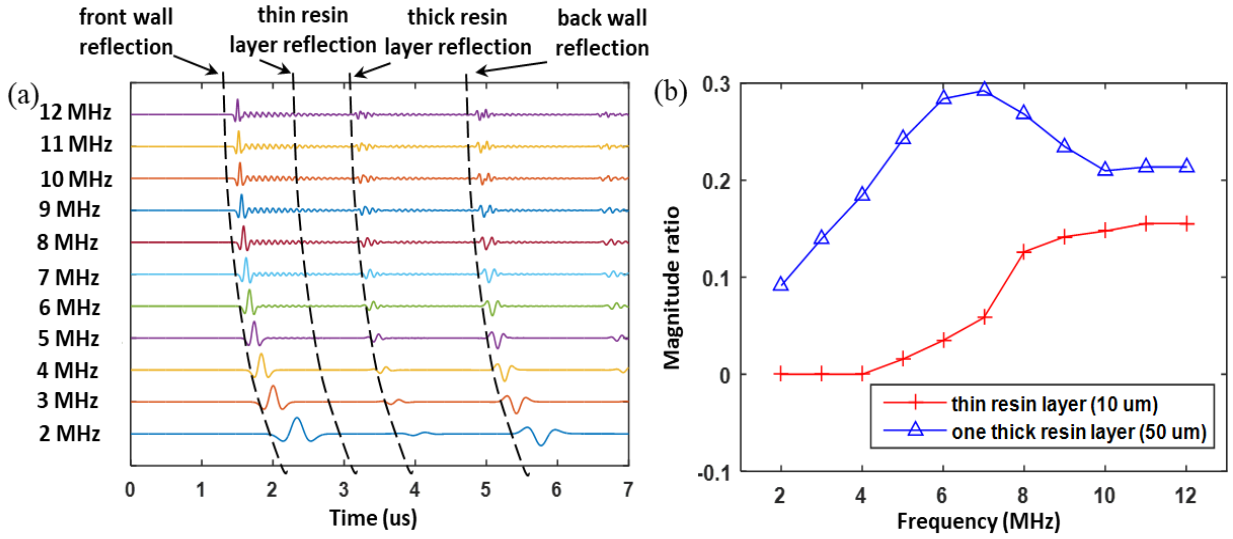

Figure 4. (a) PE signals from flat composite model with one 50 μm thick resin layer between Layers 20 and 21 and (b) its signal magnitude ratio of resin layer reflection to front wall reflection in flat composite model

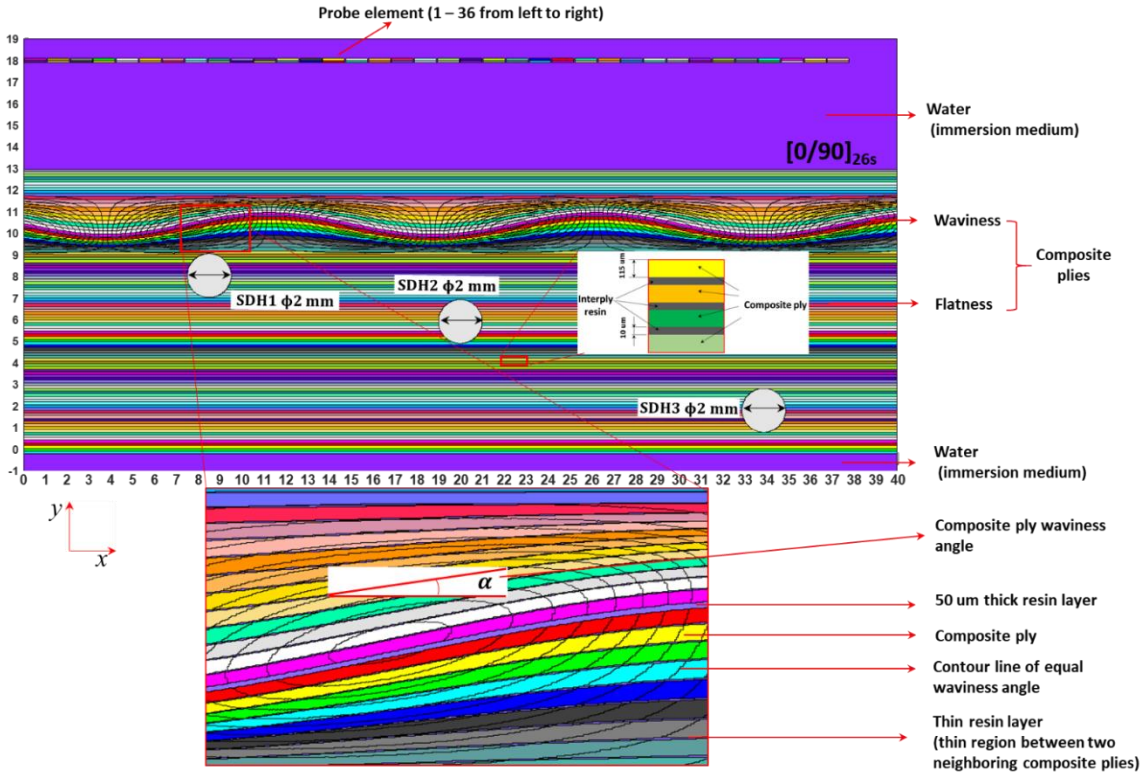

Figure 5. Composite models with SDHs and out-of-plane waviness.

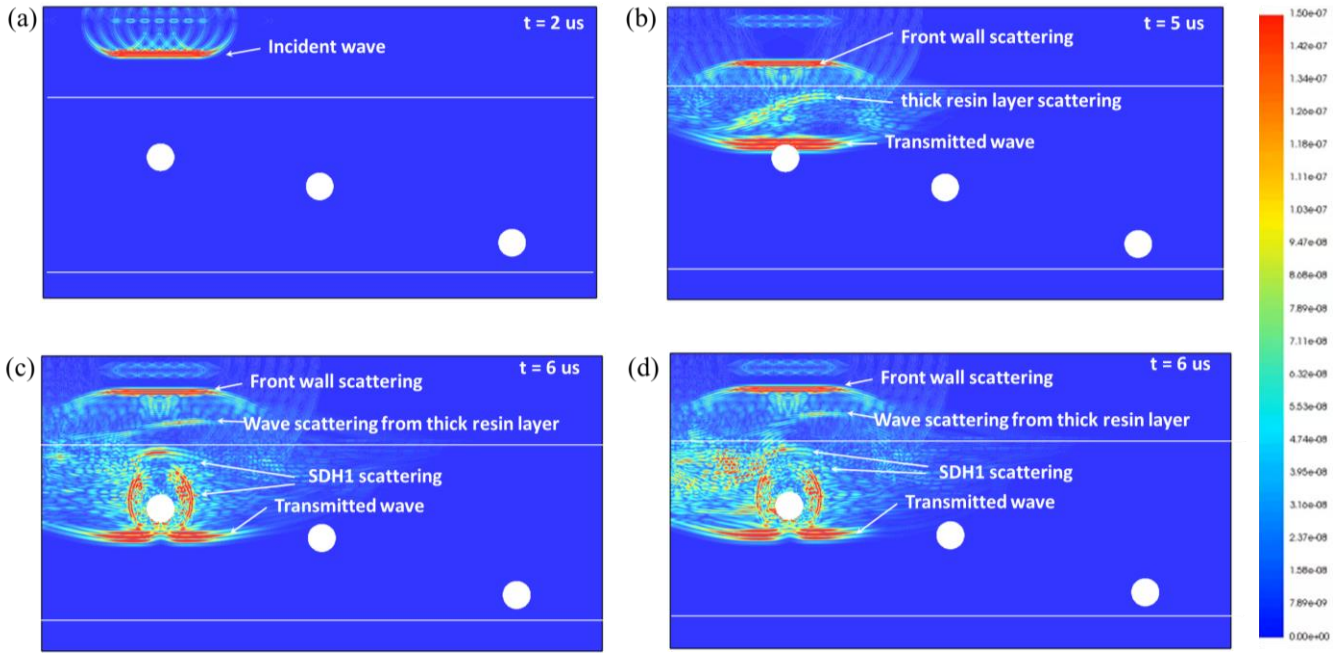

Figure 6. Simulated velocity magnitude contour in wavy composite with one thick resin layer 50 μm in thickness at $f = 5\ MHz$ (a) -(c) maximum waviness angle 12° and (d) maximum waviness angle 20°.

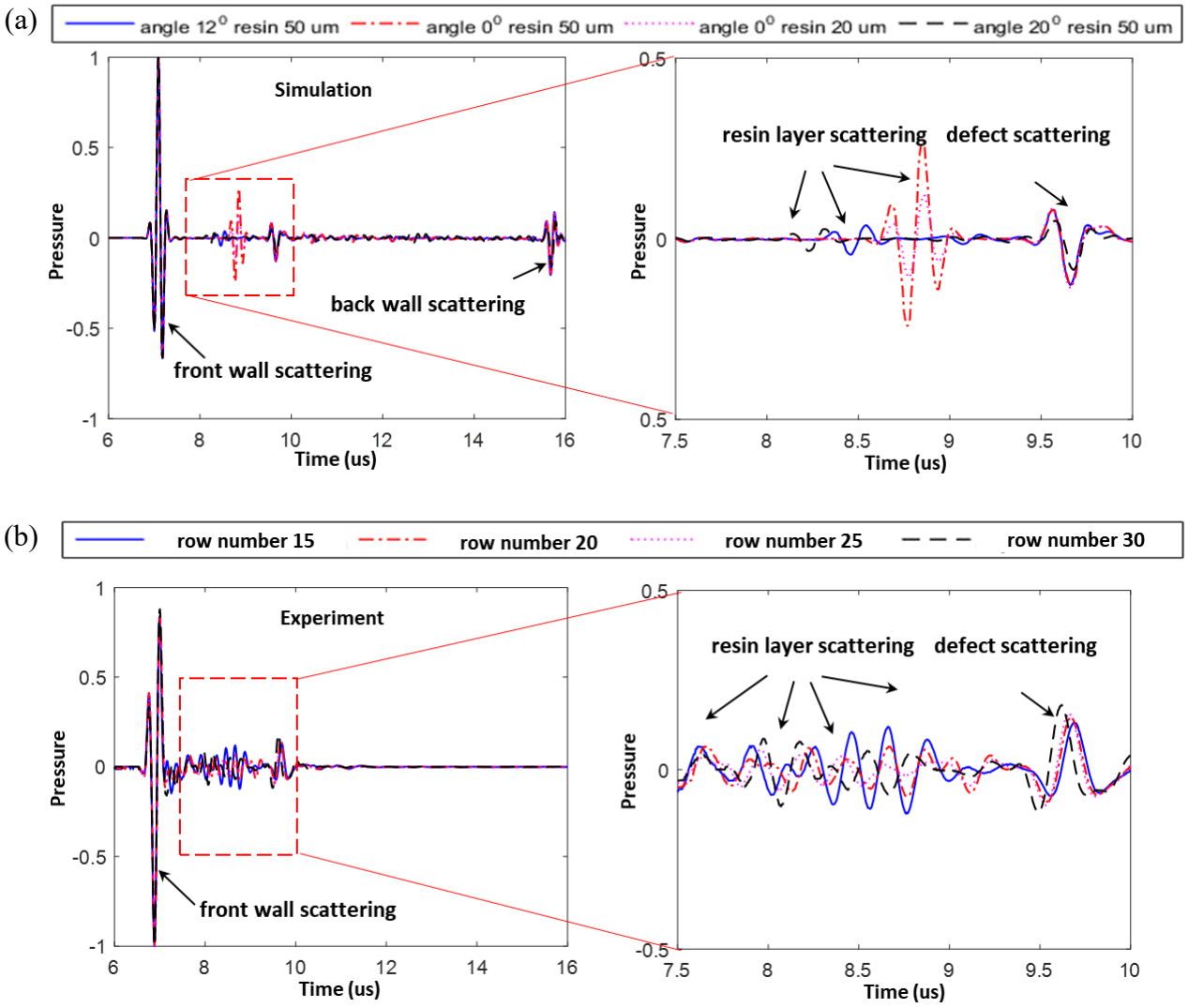

Figure 7. A-scan signals corresponding to SDH1 in (a) numerical simulation and (b) experimental testing.

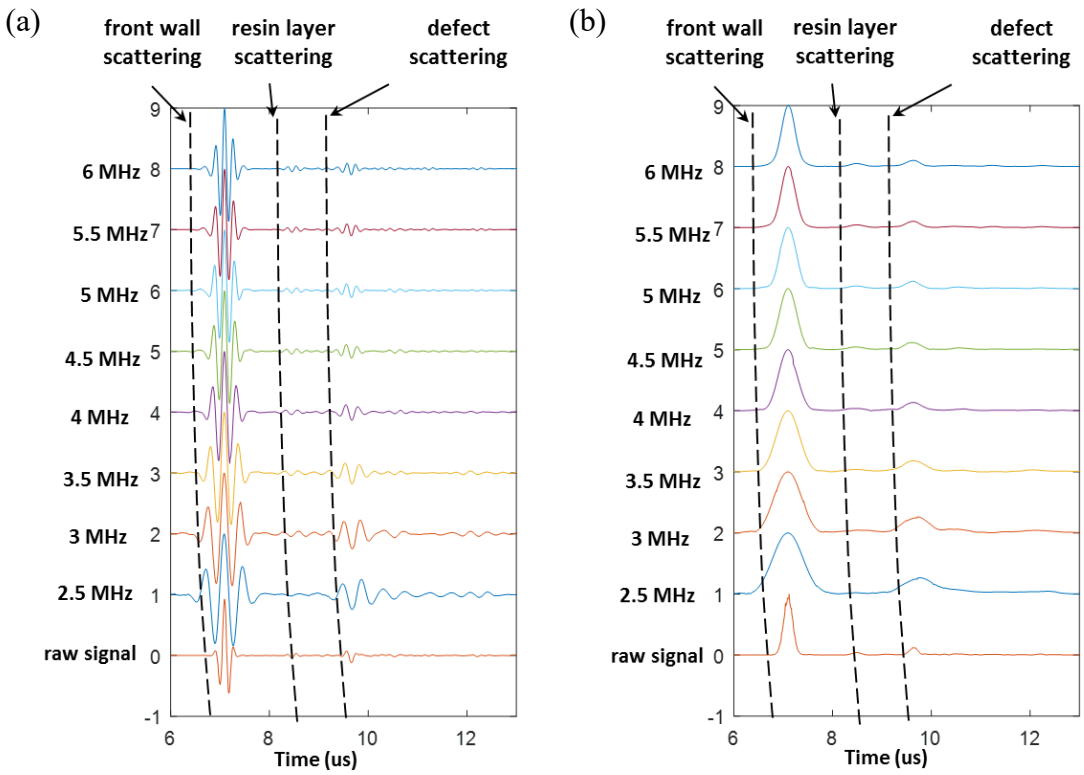

Figure 8. (a) Simulated normalized time-domain waveform and (b) simulated wave packet contour of the raw wave signal with a center frequency of 5 MHz and filtered signals with different center frequencies.

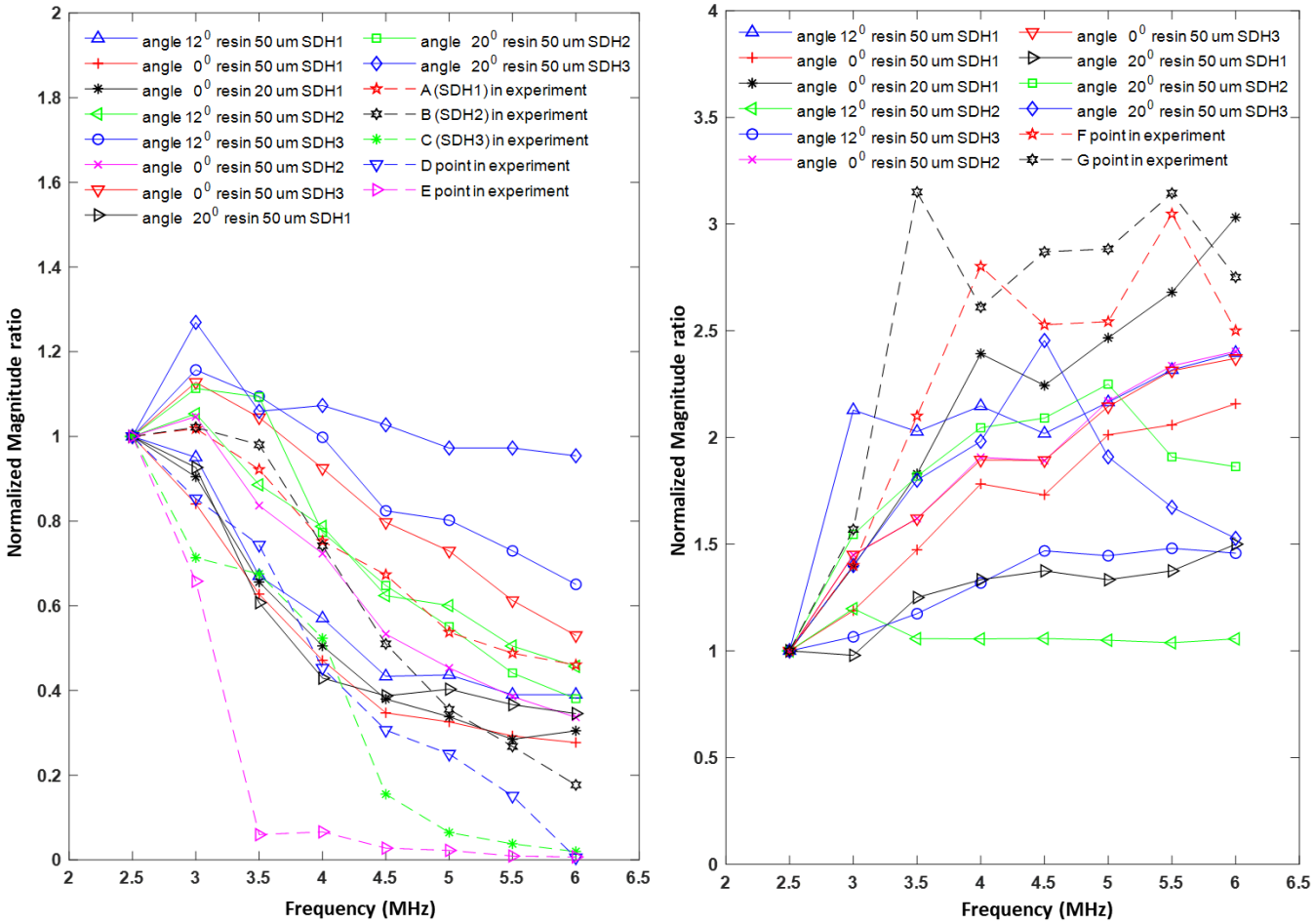

Figure 9. Normalized Magnitude ratio of (a) thick resin layerscattering and, (b) SDH scattering to the front wall scattering when the filtering central frequency increases from 2.5 MHz to 6 MHz.

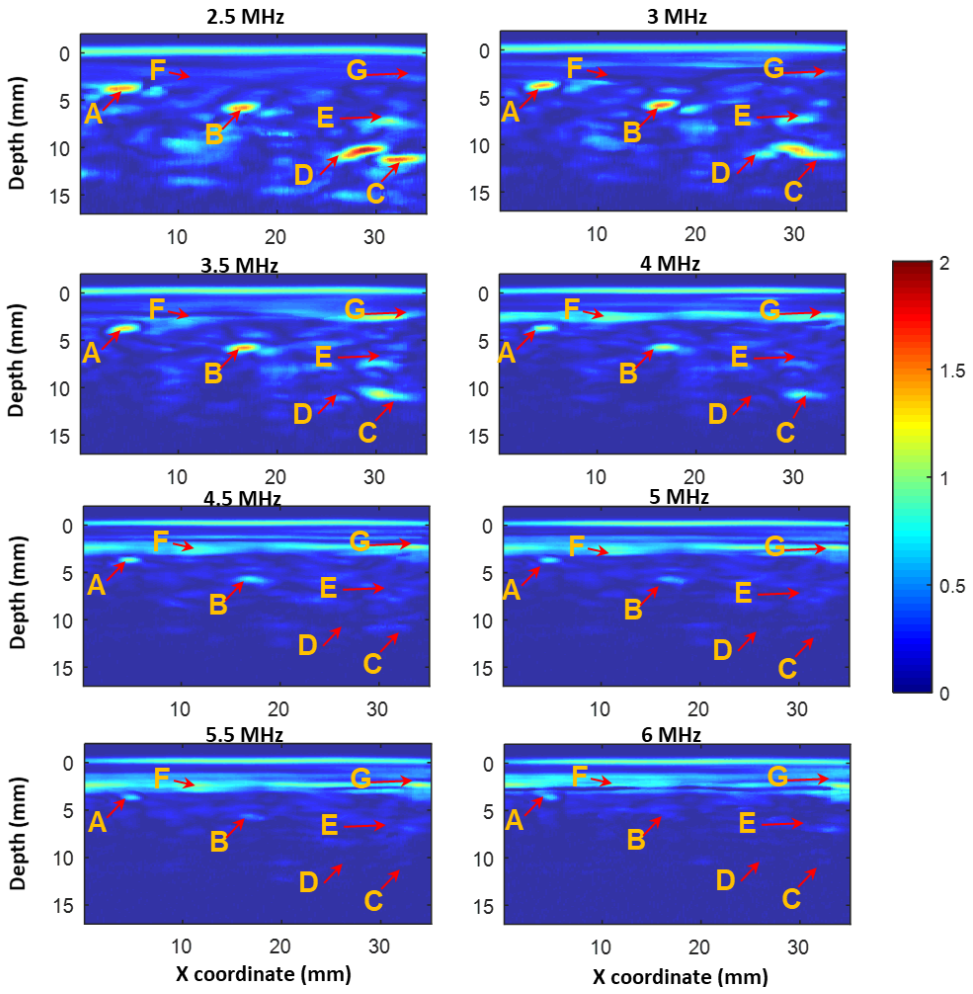

Figure 10. Experimental B-scan images of the region with three SDHs with filtering central frequency from 2.5 MHz to 6 MHz.

Table 1 Material parameter of composite ply, resin, and water.

Constituent	Density (kg/m^3)	Stiffness-related parameter
Composite ply	1560	Stiffness matrix (GPa): $\begin{bmatrix} 165.24 & 6.63 & 6.63 & 0 & 0 & 0 \\ & 14.32 & 6.39 & 0 & 0 & 0 \\ & & 14.32 & 0 & 0 & 0 \\ & *sym* & & 3.96 & 0 & 0 \\ & & & & 5.17 & 0 \\ & & & & & 5.17 \end{bmatrix}$
Matrix	1301	Young's modulus (GPa): 4.67 Poisson's ratio: 0.37
Water	1000	Longitudinal wave velocity (m/s): 1496

Table 2 Geometry parameter of composite with waviness.

Parameter	A (mm)	λ_x (mm)	λ_y (mm)	u_y (mm)	tkn (mm)	Ply number	Ply orientation
Value	0/0.50/0.86	15	3	10.5	13.05	104	$[0\ 90]_{26s}$